

AD-A194 225

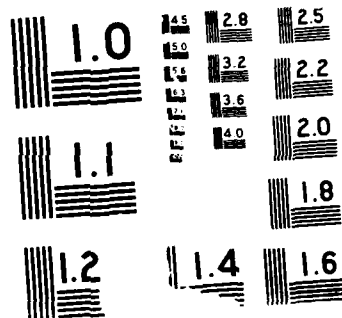
DRAG REDUCTION FOR EXTERNAL AND INTERNAL BOUNDARY  
LAYERS USING RIBBLETS AND POLYMERS(U) NAVAL OCEAN  
SYSTEMS CENTER SAN DIEGO CA L W REIDY ET AL FEB 88

1/1

UNCLASSIFIED

F/G 20/4

NL



AD-A194 225

## DOCUMENTATION PAGE

1a. REPORT SECURITY CLASSIFICATION UNCLASSIFIED		1b. RESTRICTIVE MARKINGS													
2a. SECURITY CLASSIFICATION AUTHORITY		3. DISTRIBUTION/AVAILABILITY OF REPORT  Approved for public release; distribution is unlimited.													
2b. DECLASSIFICATION/DOWNGRADING SCHEDULE															
4. PERFORMING ORGANIZATION REPORT NUMBER(S)		5. MONITORING ORGANIZATION REPORT NUMBER(S)													
6a. NAME OF PERFORMING ORGANIZATION Naval Ocean Systems Center	6b. OFFICE SYMBOL (if applicable) NOSC	7a. NAME OF MONITORING ORGANIZATION Naval Ocean Systems Center													
6c. ADDRESS (City, State and ZIP Code)  San Diego, California 92152-5000		7b. ADDRESS (City, State and ZIP Code)  San Diego, California 92152-5000													
8a. NAME OF FUNDING/SPONSORING ORGANIZATION Director of Naval Laboratories	8b. OFFICE SYMBOL (if applicable) DNL	9. PROCUREMENT INSTRUMENT IDENTIFICATION NUMBER													
8c. ADDRESS (City, State and ZIP Code)  Space and Naval Warfare Systems Command Independent Research Programs (IR) Washington, DC 20360		10. SOURCE OF FUNDING NUMBERS <table border="1"><thead><tr><th>PROGRAM ELEMENT NO.</th><th>PROJECT NO.</th><th>TASK NO.</th><th>AGENCY ACCESSION NO.</th></tr></thead><tbody><tr><td>61152N</td><td>ZT23</td><td>RR0000101</td><td>DN487 753</td></tr></tbody></table>		PROGRAM ELEMENT NO.	PROJECT NO.	TASK NO.	AGENCY ACCESSION NO.	61152N	ZT23	RR0000101	DN487 753				
PROGRAM ELEMENT NO.	PROJECT NO.	TASK NO.	AGENCY ACCESSION NO.												
61152N	ZT23	RR0000101	DN487 753												
11. TITLE (include Security Classification)  Drag Reduction for External and Internal Boundary Layers Using Riblets and Polymers															
12. PERSONAL AUTHOR(S)  L.W. Reidy and G.W. Anderson															
13a. TYPE OF REPORT Professional paper/speech	13b. TIME COVERED FROM Jan 1988 TO Jan 1988	14. DATE OF REPORT (Year, Month, Day) February 1988	15. PAGE COUNT												
16. SUPPLEMENTARY NOTATION															
17. COSATI CODES <table border="1"><thead><tr><th>FIELD</th><th>GROUP</th><th>SUB-GROUP</th></tr></thead><tbody><tr><td></td><td></td><td></td></tr><tr><td></td><td></td><td></td></tr><tr><td></td><td></td><td></td></tr></tbody></table>		FIELD	GROUP	SUB-GROUP										18. SUBJECT TERMS (Continue on reverse if necessary and identify by block number)  riblet film boundary layer drag-reducing polymer	
FIELD	GROUP	SUB-GROUP													
19. ABSTRACT (Continue on reverse if necessary and identify by block number)  Two hydrodynamic experiments have been conducted to measure the drag reduction using riblets in turbulent boundary layers. The first was an external boundary layer experiment using a flat plate in a water tunnel, and the second was an internal boundary layer experiment using a 6-inch diameter pipe. Both experiments used adhesive-backed, vinyl, riblet film, manufactured by the 3M Company, with height and spacing of the symmetric v-grooves equal to 0.003 inch. For the flat plate test, free stream velocities ranged from 6.5 ft/sec to 20 ft/sec, and $Re_\delta$ ranged from 1260-7040. The results are in good agreement with aerodynamic data, and show a maximum drag reduction of $8.1\% \pm 2.5\%$ at $s^+ = 13.1$ . Much larger percentages of friction reduction (approximately three times as much) were measured with riblets in the pipe. When a drag-reducing polymer solution was used in conjunction with the riblets in the pipe flow, the total drag reduction was approximately equal to the sum of the drag reductions of the two techniques used separately, with some dependence on Reynolds number. Before these pipe flow results can be extended to general situations, further experiments are needed to investigate the boundary layer transition from smooth to riblet surface.  Presented at AIAA 26th Annual Aerospace Sciences Meeting/Fluid Dynamics, 11-14 January 1988, Reno, NV.															
20. DISTRIBUTION/AVAILABILITY OF ABSTRACT <input type="checkbox"/> UNCLASSIFIED/UNLIMITED <input checked="" type="checkbox"/> SAME AS RPT <input type="checkbox"/> DTIC USERS		21. ABSTRACT SECURITY CLASSIFICATION UNCLASSIFIED													
22a. NAME OF RESPONSIBLE INDIVIDUAL L.W. Reidy		22b. TELEPHONE (include Area Code) (619) 553-1610	22c. OFFICE SYMBOL Code 634												

# AIAA'88

**AIAA-88-0138**

## **Drag Reduction for External and Internal Boundary Layers Using Riblets and Polymers**

L.W. Reidy and G.W. Anderson,  
Naval Ocean Systems Center, San  
Diego, CA

Accession For	
NTIS GRA&I	<input checked="" type="checkbox"/>
DTIC TAB	<input type="checkbox"/>
Unannounced	<input type="checkbox"/>
Justification	
By _____	
Distribution/	
Availability Codes	
Dist	Avail and/or Special
A-1	

## **AIAA 26th Aerospace Sciences Meeting**

January 11-14, 1988/Reno, Nevada

For permission to copy or republish, contact the American Institute of Aeronautics and Astronautics  
370 L'Enfant Promenade, S.W., Washington, D.C. 20024

88 4 32 06 5

# DRAG REDUCTION FOR EXTERNAL AND INTERNAL BOUNDARY LAYERS USING RIBLETS AND POLYMERS

Laurel W. Reidy and Greg W. Anderson  
Naval Ocean Systems Center  
San Diego, California

## Abstract

Two hydrodynamic experiments have been conducted to measure the drag reduction using riblets in turbulent boundary layers. The first was an external boundary layer experiment using a flat plate in a water tunnel, and the second was an internal boundary layer experiment using a 6-inch diameter pipe. Both experiments used adhesive-backed, vinyl, riblet film, manufactured by the 3M Company, with height and spacing of the symmetric v-grooves equal to 0.003 inch. For the flat plate test, free stream velocities ranged from 6.5 ft/sec to 20 ft/sec, and  $Re_\theta$  ranged from 1260 - 7040. The results are in good agreement with aerodynamic data, and show a maximum drag reduction of  $8.1\% \pm 2.5\%$  at  $s^+ = 13.1$ . Much larger percentages of friction reduction (approximately three times as much) were measured with riblets in the pipe. When a drag-reducing polymer solution was used in conjunction with the riblets in the pipe flow, the total drag reduction was approximately equal to the sum of the drag reductions of the two techniques used separately, with some dependence on Reynolds number. Before these pipe flow results can be extended to general situations, further experiments are needed to investigate the boundary layer transition from smooth to riblet surfaces.

## Nomenclature

$A$  = Pipe cross-sectional area  
 $C_f$  = Local Skin Friction Coefficient =  $\frac{2\tau_w}{\rho U_\infty^2}$   
 $D$  = Drag force =  $b\rho U_\infty^2\theta$   
 $\%DR$  = Percentage Drag Reduction  
 $H$  = Shape factor =  $\frac{\delta^*}{\theta}$   
 $L$  = Distance along pipe length for  $\Delta P$   
 $\Delta P$  = Pressure drop over the pipe length  $L$   
 $Re_\theta$  = Momentum thickness Reynolds number  
 $= \frac{U_\infty\theta}{\nu}$   
 $Re_d$  = Pipe diameter Reynolds number =  $\frac{Vd}{\nu}$   
 $Re_x$  = x-distance Reynolds number =  $\frac{U_\infty x}{\nu}$   
 $U_e$  = Edge velocity =  $u(\delta)$   
 $U_\infty$  = Free stream velocity

$\bar{V}$  = Bulk velocity  
 $b$  = Test plate width  
 $d$  = Pipe diameter  
 $f$  = Darcy friction factor =  $4C_f$   
 $h$  = Riblet groove height  
 $h^+$  = Riblet groove height in wall units =  $\frac{hu^*}{\nu}$   
 $\dot{m}$  = Mass flow rate  
 $r$  = Pipe radius  
 $s$  = Riblet groove spacing  
 $s^+$  = Riblet groove spacing in wall units =  $\frac{su^*}{\nu}$   
 $u(y)$  = x-direction mean velocity  
 $u'(y)$  = Fluctuating component of x-direction velocity (standard deviation)  
 $u^+$  = Velocity in wall units =  $\frac{u}{u^*}$   
 $u^*$  = Friction velocity =  $U_\infty\sqrt{\frac{C_f}{2}}$ ;  $\bar{V}\sqrt{\frac{f}{8}}$   
 $x$  = Distance from leading edge of plate in flow direction  
 $y$  = Distance above the plate  
 $y^+$  =  $y$  in wall units =  $\frac{yu^*}{\nu}$   
 $\delta$  = Boundary layer thickness; equal to  $y$  where  $u=0.999U_\infty$   
 $\delta^*$  = Boundary layer displacement thickness  
 $= \int_{y=0}^{\infty} (1 - \frac{u(y)}{U_\infty}) dy$   
 $\theta$  = Boundary layer momentum thickness  
 $= \int_{y=0}^{\infty} \frac{u(y)}{U_\infty} (1 - \frac{u(y)}{U_\infty}) dy$   
 $\mu$  = Viscosity of water  
 $\nu$  = Kinematic viscosity of water =  $\frac{\mu}{\rho}$   
 $\rho$  = Density of water  
 $\tau_w$  = Wall shear stress =  $\mu(\frac{du}{dy})_w$   
 Subscripts:  
 $c$  = control surface (smooth vinyl)  
 $l$  = leading edge of test surface  
 $r$  = riblet surface  
 $t$  = trailing edge of test surface  
 $w$  = at the wall

## 1. INTRODUCTION

One approach to achieving drag reduction is by altering the structure of the turbulent boundary layer such that the skin friction over the surface is reduced. Reference 1 is a review of many

methods that use this approach. Modification of the body surface using streamwise grooves, or riblets, is one of these methods. A few percentage points of net drag reduction will provide substantial cost savings or improved speed and endurance capabilities for aerodynamic and hydrodynamic applications.

In 1979, Michael Walsh of NASA Langley began a series of wind tunnel tests on streamwise micro-grooves [2,3,4]. After testing a wide range of groove geometries on flat plates, he determined that sharply peaked triangular v-grooves, with height and spacing equal to 10 - 15 wall units, produced the optimum drag reduction of about 9%. Frank Marentic of the 3M Company recognized an opportunity for manufacturing riblets in small groove sizes for high Reynolds number applications. Currently, 3M has the capability of manufacturing adhesive-backed, vinyl riblet films in a variety of groove sizes.

Based on Walsh's aerodynamic results, others have tested flat plates with v-groove surfaces in water. These include a water channel test at a flow velocity of approximately 0.3 m/sec ( $Re_\theta$  up to 1350) using grooves machined in plexiglas. This test, performed at Lehigh University [5], showed drag reduction results very similar to Walsh's results. A separate but very similar study at Lockheed-Georgia [7] was not able to measure drag accurately enough to confirm these results. In 1985, 3M riblets were applied to rowing shells and tested in a towing tank at David Taylor Research Center. The results were widely variable, and tended to indicate a degradation of the riblets from one day to the next. From a series of rowing tests, however, it was determined that the vinyl riblets reduced the boat drag by 2% [8].

The Lehigh University facility was also used for flow visualization of the boundary layer, the results of which provide a basis for a discussion of how riblets cause drag reduction [5,6]. The increased surface area of a grooved surface compared to a smooth surface may intuitively indicate an increase, rather than decrease, in skin friction. It is postulated, however, that the sharp peaks of the v-grooves serve to break up the streamwise vortices, inhibiting low-speed streak formation. In this way, the turbulent momentum exchange and skin friction would be reduced. A different explanation is that the flow in the troughs is very slow-moving, so that even if the wall shear stress is increased at the peaks of the grooves, it is very much decreased in the valleys, causing a net decrease in the skin friction.

The only known experiment to use streamwise grooves in pipeflow was conducted by Nitschke in Germany using fully-developed air flow [9]. Rounded peaks with flat valleys were

used, rather than sharply peaked v-grooves. A maximum drag reduction of 3% was calculated using pressure drop measurements over a length of 120 pipe diameters. Drag reduction was obtained for  $s^+ = 8$  to  $s^+ = 30$ .

The present work applies 3M v-groove riblets in the turbulent boundary layer region of external and internal water flows. For the external boundary layer test, riblets were applied to a flat plate in a high-speed water tunnel. The skin friction drag is calculated from velocity profile data. Spanwise measurements both upstream and downstream of the riblet surface are performed to ensure that the results are not biased by a spanwise non-uniformity. For the internal boundary layer test, riblets were applied to the inside of a 6-inch diameter pipe. Mass flowrate and pressure drop measurements were used to calculate the friction factor. This paper is divided into two sections, one describing the external flow experiment, and the other describing the internal flow experiment.

## II. EXTERNAL FLOW EXPERIMENT

### Experimental Apparatus

**Test Facility.** The experiment was conducted in the Naval Ocean Systems Center high speed, open jet, recirculating water tunnel. The test section is 1 m long, with a 0.31 m diameter jet, and a turbulence level,  $u'/U_\infty$ , less than 0.25% for speeds up to 12 m/sec. The flat plate model was mounted on longitudinal supports, outside of the jet, in a horizontal position along the centerline. The test plate and its leading edge were separately constructed from type 302 stainless steel. The flat plate is 19.0 mm thick and 0.58 m wide, with an overall length of 0.86 m. The leading edge piece has a streamwise length of 0.15 m and a width of 0.30 m and was machined to include a rounded edge with a 1.6 mm high forward facing step. The step was designed to act as a tripping device, and the leading edge was placed in the water tunnel's contraction section in order to obtain as long a test plate as possible. A diagram of the test plate is shown in Figure 1.

Velocity field measurements were made using a TSI Laser Doppler Velocimeter (LDV) mounted on a three-dimensional traverse with numerically-controlled positioning. The LDV was operated in the backward scatter mode using a 1 W Argon-Ion laser. The transmitting and receiving optics were positioned at an angle of approximately one degree (pointing towards the plate) instead of the usual arrangement of the system parallel to the test plate. This configuration reduces the interference between the laser beams

and the flat plate enabling velocities to be measured as close as 0.05 mm from the plate. Velocities at 20 or more y-locations were measured for each boundary layer profile.

**Riblet Geometry.** The vinyl riblet film used in the tests was manufactured by the 3M Company. A single geometry of v-groove riblets was tested. The grooves have height,  $h$ , equal to spacing,  $s$ , equal to 0.0762 mm (0.003 inch). The total film thickness measured from the bottom of the vinyl sheet to the peaks of the grooves is 0.1524 mm. A plain vinyl film, 0.0762 mm thick, was used as a control surface. Since the vinyl riblets were originally developed for use in air, photomicrographs were taken of the materials after soaking overnight in water. The photographs showed no swelling or visible changes between the water-soaked and dry riblets. A photomicrograph of the riblet cross-section looking in the flow direction is shown in Figure 2. When drag measurements were made, the riblets had been submerged in water for up to a total of 22 hours. No degradation of drag reduction performance was observed.

A sheet of riblet film, 0.305 m wide by 0.481 m in the streamwise direction, was attached to the flat plate with the leading edge of the film at  $x=0.184$  m and the trailing edge at  $x=0.665$  m. For control measurements, the plain vinyl of the same dimensions was attached in the same location. The adhesive film, either riblets or smooth vinyl, will be referred to as the test surface in this report. The location of the test surface on the test plate is shown in Figure 1.

**Baseline Tests.** Velocity measurements with the control surface in place were performed to ensure the presence of a zero pressure-gradient, fully turbulent boundary layer in the measurement region. The velocity profile data shown in Figure 3 were obtained at  $x=0.320$  m, 0.524 m, 0.651 m, and 0.778 m, and are presented in terms of  $u/U_e$  vs.  $y/\theta$ . The collapse of the data on a single curve represents good similarity of the profiles over the measurement region. Figure 4 shows a profile of  $u'/U_e$ , the fluctuating streamwise velocity component, obtained at  $x=0.216$  m, non-dimensionalized by the edge velocity, and compares it to the generally-accepted flat plate data reported by Klebanoff [10].

In addition to the  $(y/\theta, u/U_e)$  profiles, plots of  $(u^+, y^+)$  were made using the skin friction coefficient,  $C_f$ , calculated from empirical relationships. A typical  $(u^+, y^+)$  plot is shown in Figure 5, where  $C_f$  was calculated using the Ludweig-Tillman relationship,

$$C_f = 0.246(10)^{-0.678H} Re_\theta^{-0.208},$$

where the values of  $\delta^*$ ,  $\theta$ , and  $H$  were obtained by integrating the experimental velocity profiles. The

measured  $(u^+, y^+)$  profile compares favorably to the universal logarithmic profile, shown in Figure 5, given by,

$$u^+ = \frac{1}{0.4} \ln y^+ + 5.0.$$

The velocity point that is closest to the wall, at  $y = 0.05\text{mm} \pm 0.02\text{mm}$ , is the only point in the viscous sublayer region ( $u^+ = y^+$  region).

The skin friction coefficient from the Ludweig-Tillman equation was also used to calculate the riblet size in wall units,  $h^+$  and  $s^+$ . Note that for the riblets tested,  $h^+ = s^+$  since  $h=s$ . To calculate  $s^+$ , velocity profiles were measured 4 mm upstream of the leading edge of the test surface, at  $x=0.179$  m. The local skin friction coefficient from the Ludweig-Tillman relationship, the free stream velocity, and the viscosity are used to calculate  $s^+$  from

$$s^+ = \frac{sU_\infty}{\nu} \sqrt{\frac{C_f}{2}}.$$

This technique for calculating  $s^+$  is not appropriate on or downstream of the riblet surface, because the smooth flat plate empirical relation for  $C_f$  is not applicable to the boundary layer that has been affected by riblets.

## Results

**Momentum Thickness.** Each velocity profile was integrated to produce momentum thickness,  $\theta$ . A comparison of momentum thicknesses is the basis for the drag reduction measurements of this study. In order to compare a momentum thickness downstream from the riblet surface to one downstream from the plain vinyl surface, some adjustments must be made, because the water temperature and free stream velocity will not be exactly the same for the two measurements made on different days. The power-law flat plate approximation,

$$Re_\theta = 0.03497 Re_x^{4/5},$$

can be rearranged to,

$$\theta = 0.03497 \frac{x}{Re_x^{1/5}} = 0.03497 \frac{\nu^{1/5}}{U_\infty^{1/5}} x^{4/5}.$$

In order to compare two momentum thicknesses at the same  $x$ -location measured on different days with nearly the same values of  $\nu$  and  $U_\infty$ , all measured  $\theta$ 's are adjusted to the same  $\nu$  and  $U_\infty$ . All measurements were adjusted to a viscosity of  $1.05 \times 10^{-6} \text{m}^2/\text{sec}$ , which corresponds to  $18^\circ\text{C}$ . The measurements are also adjusted to the exact free stream velocity that was attempted, either 2.0, 3.0, 3.5, 4.0, 4.5, 5.0, or 6.0 m/sec. The equation used to adjust momentum thicknesses, then, is

$$\frac{\theta_{\text{adjusted}}}{\theta_{\text{measured}}} = \left( \frac{\nu_{18C}}{\nu_{\text{measured}}} \right)^{1/5} \left( \frac{U_{\infty, \text{measured}}}{U_{\infty, \text{exact}}} \right)^{1/5}$$

Figure 6 is a plot of adjusted momentum thickness for  $U_{\infty} = 3.5$  m/sec. Five spanwise values at  $x = 0.70$  m (35 mm downstream from the test surfaces) are shown for comparing the riblet surface to the control surface. One can see the effect of the riblet film in reducing the momentum thickness. The increase in momentum thickness at spanwise distances from the plate centerline ( $z=0.0$ ) is due to the spreading of the jet in the open jet test section. At all of the spanwise measuring stations, the drag-reducing effect of the riblets can be seen.

**Drag Calculations.** The drag on the flat plate was calculated using

$$D = b\rho U_{\infty}^2 \theta$$

The drag reduction over the test surface portion of the plate can be represented as

$$\%DR = \frac{(D_t - D_l)_c - (D_t - D_l)_r}{(D_t - D_l)_c}$$

where the subscripts are  $t$  = to the trailing edge of the test surface,  $l$  = to the leading edge of the test surface,  $c$  = control surface,  $r$  = riblet surface. Recognizing that if adjusted momentum thicknesses, as described in the previous section, are used so that  $b\rho U_{\infty}^2$  is a constant, and that the drag upstream of the leading edge of the test surface is the same for riblet and control surfaces ( $D_{l,c} = D_{l,r}$ ), the drag reduction equation reduces to

$$\%DR = \frac{\theta_{t,c} - \theta_{t,r}}{\theta_{t,c} - \theta_l}$$

Trailing edge momentum thicknesses were measured at  $x = 0.700$  m, which is 35 mm downstream from the trailing edge of the test surface. Velocity profiles closer to the trailing edge are not used because the small step down from the film to the plate may affect the profile shape. However, for the purpose of calculating drag reduction over the length of the test surface film only, the momentum thickness is adjusted so that it corresponds to  $\theta$  at  $x=0.665$  m, the actual trailing edge of the test surface, using the flat plate approximation relating  $Re_x$  and  $Re_{\theta}$  given in the previous section. The same method was used to adjust momentum thicknesses measured 4 - 15 mm upstream of the test surface to correspond to the leading edge. This flat plate approximation may not be perfectly accurate for the region downstream from the test surface that has been affected by riblets, but it is more accurate than treating the area between the trailing edge and the measuring station as if it were covered with riblets. In addition, these adjustments to  $\theta$  are very small compared to the change in  $\theta$  over the 481 mm length of the test surface.

The drag reduction results are shown in Figure 7 as a function of riblet size in wall units. The values of  $s^+$  correspond to the leading edge of the test surface;  $s^+$  will increase by about 9% from the leading edge to the trailing edge of the test surface. The drag reduction percentages in Figure 7 are calculated from the momentum thickness measurements on the plate centerline ( $z=0.0$ ). The maximum measured drag reduction is 8.1%, which occurred for  $s^+=13.1$ . If a curve is drawn between data points, the region of positive drag reduction is seen to extend from approximately  $s^+=7$  to  $s^+=20$ . Outside of this range, the riblets will be likely to increase, rather than decrease, the surface drag. These results are in good agreement with the bulk of data for v-groove surfaces in aerodynamic and hydrodynamic experiments.

The uncertainties in the measured quantities, velocity and y-position, were used to calculate an uncertainty in momentum thickness of  $\pm 1.1\%$  of the measured value. Based on this, the error bands on percent drag reduction (%DR), shown in Figure 7, range from  $\pm 2.5\%$  to  $\pm 2.9\%$ , depending on the Reynolds number. The uncertainty analysis also points out that as the x-direction length of riblet material is decreased, the uncertainty in percent drag reduction increases. For this reason, the maximum possible length of riblet material was used.

**Velocity and Turbulence Profiles.** Profiles of the mean and fluctuating components of the streamwise velocity were measured over the riblet film, as well as downstream from the film. However, because of the uncertainty in choosing a  $y=0$  position for the grooved surface, the profiles over the riblets are not included here. Profiles measured at  $x=0.70$  m, which is 35 mm or approximately 2.56 downstream from the trailing edge of the test surfaces, are shown in Figures 8 and 9. The mean velocity profile (Figure 8) shows a region of increased velocity downstream from the riblets compared to the smooth test surface for  $y/\theta$  from 0.04 - 0.6. For  $y/\theta$  greater than 0.6, the velocities downstream from the riblets are approximately equal to the velocities downstream from the smooth surface.

The corresponding turbulence profile (Figure 9) does not present as clear of a picture, but it does illustrate some observed trends. The scatter associated with the rms measurements is particularly large in the near-wall region, and is probably due to interference of the laser with the test plate. For  $y/\theta$  from 0.08 - 0.4,  $u'/U_e$  is suppressed for the riblet case as compared to the smooth test surface. For  $y/\theta$  from 0.4 - 1.0,  $u'/U_e$  for the riblet case tends to be larger than or equal to that for the smooth test surface case, and for  $y/\theta$  greater than 1.0,  $u'/U_e$  measurements for the two cases are

coincident.

## II. INTERNAL FLOW EXPERIMENT

### Background

There are two purposes for the pipe flow experiments presented in this paper. First, improvements for piping systems are sought by reducing friction losses. Second, this experiment provides a comparison between pipe flow and flat plate drag reduction experiments using the same riblet surfaces. This sort of direct comparison between drag reduction for internal and external boundary layers is of interest, since it is not clear that the percentage friction reduction in pipes will be the same as for flat plates when using riblets and/or polymers.

### Experimental Apparatus

Test Facility. The experiment was conducted at the Morris Dam Test Range Facility in Azusa, California, which is a part of the Naval Ocean Systems Center. A schematic of the pipe flow apparatus is shown in Figure 10. The pipeline is gravity-fed from a 45,000 gallon tank situated on a hill, providing 91 feet of available head. The test pipe consists of 85 feet of seamless, Schedule 40, stainless steel pipe, honed as one unit to an inside diameter of 6.15 inch. The specified finish for the inside of the pipe was 32  $\mu$ in, and when new in 1983, the roughness was measured as 20  $\mu$ in. The test section with riblets was located 61 feet (119 diameters) downstream from the entrance to the test pipe. Bulk velocities from 2.6 - 55 ft/sec are attainable.

Measurements of differential pressure, flowrate, and water temperature were performed. The pressure drop was measured over a 2-foot length of pipe. Four Validyne DP15 Variable Reluctance Differential Pressure Transducers with full-scale capabilities of 0.125, 0.2, 0.5, and 2.0 psi were calibrated with a water manometer then connected to the pipe. Automatically controlled solenoids determined which transducer was appropriate. Three 1/16-inch diameter pressure tap holes located at 120° intervals were combined for a circumferential average at each of the two measuring stations along the pipe axis. Validyne CD18 carrier demodulators were used in conjunction with each pressure transducer for signal calibration and conditioning. Flowrates up to 20,000 lb/min were measured using a Micro-Motion D600 mass flow meter. Flowrates from 20,000 - 45,000 lb/min were calculated from the drop in the tank level and the elapsed time. Temperature was measured with a thermocouple inserted at the

entrance to the 6-inch diameter pipe length, monitored with a Validyne signal conditioner.

Riblet Application. The v-groove vinyl riblets were manufactured and provided by the 3M Company, through Mr. Frank Marentic. A photomicrograph showing the riblet cross-section is shown in Figure 2. The riblets tested had peak height,  $h$ , equal to spacing,  $s$ , of 0.003-inch. This is the same type of riblet film as was used for the external flow experiment. A smooth film, 0.003-inch thick, without any peaks was also tested. This control surface was attached to the pipe in an identical manner as the riblet surfaces.

The vinyl riblet film was applied to the inside of the pipe test section, a 5-foot pipe length shown in Figure 11. The inner circumference of the pipe test section was covered with riblet film over the central 3 feet of length. Two pieces of riblet film were used, each one 3 ft. x 9.625 in., configured so that the grooves ran longitudinally. Differential pressure was measured over the central 2 feet of the test section.

A careful process was followed to apply the riblet film to the inside of the pipe. First, the pipe walls were sprayed with a 1% Joy detergent solution made with tap water. The two pieces of riblet film were then applied one at a time. Each piece of film was wetted with the detergent solution, then rolled lengthwise and inserted into the pipe. Once inside, it was unrolled and positioned. A special tool supplied by the 3M Company was used to squeegee the detergent solution from under the film. The tool consisted of a 0.5-inch thick piece of felt machined to the appropriate radius and attached to a 5-foot long pole. Repeated passes using this tool, gradually increasing the applied pressure, were necessary to remove all of the bubbles. After both pieces of film were attached, the pipe was set vertically to dry for 24 hours. Then the pressure tap holes through the film were made. A sharp dentists pick was used to prick a small hole from the outside, while a piece of felt was held on the inside to keep the film from pulling away from the pipe walls. A round file was then used from the inside to carefully file away the riblet film to create a clean cut. After drying, persistent bubbles could be carefully pierced with a needle and drained, though this was seldom required.

Polymer Solutions. For some of the test runs, polyacrylamide (PAM) slurry was mixed into the lake water in the 45,000 gallon tank. The slurry is injected into the filling water from a pneumatically actuated piston. The tank is equipped with large mixing vanes, which turned for approximately 4 hours before the test runs were made. In order to produce a 2 ppm solution, 830g of PAM were put into the piston. Assuming

that 5g remain stuck in the piston, then 825g are mixed into 16 ft of water. The tank holds 2723 gal/ft, which calculates to a 2ppm PAM solution.

**Data Reduction.** During a test run, the measured quantities were digitally stored at approximately 1 second intervals. At least 20 data points were collected at each flowrate before using the throttle valves to set a new flowrate. The Reynolds number and Darcy friction factor were calculated as follows.

$$Re_d = \frac{d\bar{V}}{\nu} \quad \text{where } \bar{V} = \frac{\dot{m}}{\rho A}$$

and

$$f = \Delta P \frac{2}{\rho \bar{V}^2} \frac{d}{L}$$

where  $\dot{m}$  = mass flowrate,  $\rho$  = water density,  $A$  = pipe cross-sectional area,  $\nu$  = viscosity of water (function of temperature),  $\bar{V}$  = bulk velocity,  $d$  = pipe diameter, and  $\Delta P$  = pressure drop over the distance  $L$ . The pipe diameter and cross-sectional area were adjusted for the addition of riblet and smooth films using:

$d = 6.15 \text{ in.} - 2(\text{film base thickness} + 0.5h)$ , which defines the diameter at the midpoint of the riblet peaks. This diameter correction has a very small effect on the results, because the riblet film thickness is small compared to the pipe diameter. The height and spacing of the grooves in wall units are calculated from,

$$h^+ = h \frac{u^*}{\nu} \quad s^+ = s \frac{u^*}{\nu}$$

where

$$u^* = \sqrt{\frac{d \Delta P}{4L\rho}}$$

Since  $h$  is equal to  $s$  for the riblet geometry tested,  $h^+$  is equal to  $s^+$ . Percentage drag reduction was calculated from

$$\%DR = \frac{f_{\text{control}} - f_{\text{riblet}}}{f_{\text{control}}}$$

## Results

**Baseline.** Three different sets of riblet data were obtained in this facility, during May 1986, September 1986, and April 1987. These will be referred to in this paper as data sets 1, 2, and 3. Baseline measurements for the plain stainless steel pipe, without any film coating or polymer, were obtained each time. Because the equipment was recalibrated between data sets, and because the pipe roughness may have changed slightly between data sets, the baseline measurements are all somewhat different. For each data set, however, the baselines before and after obtaining the riblet and polymer data agreed. Baseline results were

expected to coincide with the Moody diagram [11] smooth pipe data for a roughness to diameter ratio of  $5 \times 10^{-6}$ . The results actually match the Moody diagram for a roughness to diameter ratio of approximately  $2 \times 10^{-4}$ . This may be because of roughness due to water deposits, waviness in the pipe surface, curvature in the pipe length, or pressure orifice effects.

In order to investigate the effect of the change in diameter and sudden step caused by applying the riblet film, one test during data set 1 was performed using a smooth vinyl control film (no riblet grooves), 0.003-inch thick, located in the same position in the test section as the riblet films. The corrected diameter was used to calculate the friction factor, and the results (Figure 12) are very similar to the plain stainless steel results. This demonstrates that the leading and trailing edge steps do not significantly affect the results when the pipe diameter is so large compared to the film coating thickness.

**Riblets and Polymers.** Data set 1 encompassed only the flowrates that could be measured using the MicroMotion flowmeter. In addition to the smooth control surface, the riblet surface was tested (no polymers in the water). Figure 12 is a plot of the friction factor versus Reynolds number for the riblet surface compared to the baseline and the smooth control surface. Data sets 2 and 3 used twice the flowrate range as Data set 1, and included tests using 2 ppm PAM polymers in the water, as well as the riblet coatings.

For data sets 2 and 3, the tests were performed in the following order: 1) no coatings, no polymers, 2) 0.003-inch riblets, no polymers, 3) 0.003-inch riblets, 2 ppm PAM, 4) no coatings, 2 ppm PAM, 5) no coatings, no polymers. Figures 13 and 14 present the results as friction factor vs. Reynolds number. It is apparent that all three data sets gave different results for the riblet cases. The polymer runs, without riblets, are fairly consistent though. In fact, a portion of the same polymer solution used for data set 3 was run through a 1-inch diameter pipe that is parallel to the 6-inch diameter pipe. The friction reduction results compare well for the two different set-ups, as shown in Figure 15. It was probably the fresh application of riblets for each of the data sets that produced the differences in friction reduction. Possible differences include trapped particles or bubbles, quality of riblet grooves, uneven adhesive causing spanwise waves, loose riblet film around the pressure taps, or slight variations in the location of the riblet film along the axial direction. Figure 16 shows the percentage drag reduction using riblets (no polymers) for each test plotted versus  $s^+$ . Maximum drag reductions of 22% - 28% are seen to occur for  $s^+$  in the range of 10 to 30.

The measurements using riblets and polymers together show that when both drag reduction techniques are used at once, the maximum net drag reduction is seen to be approximately the sum of the drag reductions for the polymer alone and the riblets alone. At low Reynolds numbers, however, the net drag reduction is less than the sum of the drag reductions of the two techniques alone. At high Reynolds numbers, there appears to be a synergistic effect, as the drag reduction for polymers combined with riblets is greater than the sum of the drag reductions of the two techniques used separately. The synergistic effect may occur because the riblets delay the polymer degradation caused by high shear stresses to a higher Reynolds number.

Interpretation of Pipe Flow Results. The interpretation of the pipe flow results is not as straightforward as the plots of friction factor and drag reduction imply. The equation used to calculate friction factor, based on pressure drop and bulk flowrate, assumes that there is no acceleration of the fluid. For this experiment there was no bulk acceleration, but there may be some acceleration and deceleration within the velocity profile as the boundary layer adjusts to the presence of the riblets. If this change primarily occurs in the first two boundary layer thicknesses, then this technique is valid for measuring the skin friction reduction. If, however, the boundary layer is not mostly adjusted to the new surface condition by the first pressure tap, then this method of measuring friction reduction is inappropriate. A flat plate experiment [12] has shown the boundary layer to be affected by the riblets, with an estimated drag reduction of about 6%, after only 2 or 3 boundary layer thicknesses of riblet length. Since the measured drag reductions in the present pipe flow experiment are so much larger than for flat plate experiments, one concludes that either the boundary layer is in fact not at all adjusted to the riblets after 2 boundary layer lengths, or that there is indeed greater drag reduction possible using riblets in pipes than using riblets for external flow.

Clearly, more experiments are needed to measure the skin friction reduction in pipes using riblets. Ideas for further research include the construction of a split 1-inch diameter pipe that would allow riblets to be applied inside the pipe, over a 50 diameter length. Additional tests could also be performed using the 6-inch diameter pipe, applying varying amounts of upstream riblets, up to a total of about 5 diameters upstream of the first pressure tap. Experiments of this nature are needed to quantify the skin friction reduction for pipe flow as a function of distance from the leading edge of the riblets.

## IV. CONCLUSIONS

The results of this flat plate experiment are in agreement with the bulk of other measurements of drag reduction using v-groove riblets. The findings show that the vinyl riblets manufactured by the 3M Company, which were originally developed for aerodynamic applications, will perform equally well in water. The measured drag reduction of 8% will correspond to a velocity increase of 2% for a vehicle under constant power. The riblets were quite durable, and showed no degradation in performance over the time that the experiment was conducted. Since very long duration use without inspection of the surface could be a potential problem, the most practical Navy hydrodynamic application at this time may be to short-duration vehicles. Improvements in fuel economy as well as vehicle speed are possible using this simple, passive, drag reduction system.

The results of the pipe flow experiment indicate that greater friction reduction may be possible in pipe flow, than has been measured on flat plates. More internal boundary layer work is needed, however, to understand the relationship between friction reduction and axial distance from the leading edge of the riblets.

## Acknowledgments

Dr. T. S. Mautner proposed a study of riblets and provided helpful comments throughout the project. D. E. Edmunds, A. O. Musolf, and Dr. J. J. Rohr helped gather and interpret the data. Funding was provided from the Naval Ocean Systems Center Independent Research Program, and the Office of Naval Research.

## References

1. Bandyopadhyay, P. R., "REVIEW-Mean Flow in Turbulent Boundary Layers Disturbed to Alter Skin Friction," *Journal of Fluids Engineering*, Volume 108, pp 127, June 1986.
2. Walsh, M. J., and A. M. Lindemann, "Optimization and Application of Riblets for Turbulent Drag Reduction," AIAA-84-0347, AIAA 22nd Aerospace Sciences Meeting, Reno, Nevada, January 1984.
3. Walsh, M. J., "Riblets as a Viscous Drag Reduction Technique," *AIAA Journal*, Volume 21, No. 4, pp 485, April 1983.
4. Walsh, M. J., "Drag Characteristics of V-groove and Transverse Curvature Riblets," *Viscous Flow Drag Reduction*, G. R. Hough, editor, Volume 72, Progress in Astronautics and

Aeronautics, from Symposium on Viscous Drag Reduction, Dallas, Texas, November 1979.

5. Bacher, E. V., and C. R. Smith, "A Combined Visualization-Anemometry Study of the Turbulent Drag Reducing Mechanisms of Triangular Micro-Groove Surface Modifications," AIAA-85-0548, AIAA Shear Flow Control Conference, March 1985.

6. Bacher, E. V., and C. R. Smith, "Turbulent Boundary-Layer Modification by Surface Riblets," AIAA Journal, Volume 24, No. 8, pp. 1382, August 1986.

7. Gallagher, J. A., and A. S. W. Thomas, "Turbulent Boundary Layer Characteristics Over Streamwise Grooves," AIAA-84-2185, AIAA 2nd Applied Aerodynamics Conference, August 1984.

8. Eilers, R. E., Koper, C. A., McLean, J. D., and D. W. Coder, "An Application of Riblets for Turbulent-Skin-Friction Reduction," presented at the Twelfth Annual Symposium on Sailing put on by the American Institute of Aeronautics and Astronautics and the University of Washington, Seattle, Sept. 20-21, 1985.

9. Nitschke, P., "Experimental Investigation of the Turbulent Flow in Smooth and Longitudinal Grooved Pipes," Max-Planck Institute fuer Stroemungsforschung, Goettingen, West Germany, 1983, in German, available with abstract translated, NASA TM77480, 1984.

10. Hinze, J. O., Turbulence, 2nd edition, McGraw-Hill Book Company, New York, 1974.

11. White, F. M., Viscous Fluid Flow, McGraw-Hill Book Company, New York, 1974.

12. Djenidi, L., Anselmet, F., and L. Fula-chier, "Influence of a Riblet Wall on Boundary Layers," Proceedings of Turbulent Drag Reduction by Passive Means, Royal Aeronautical Society, London, September 1987.

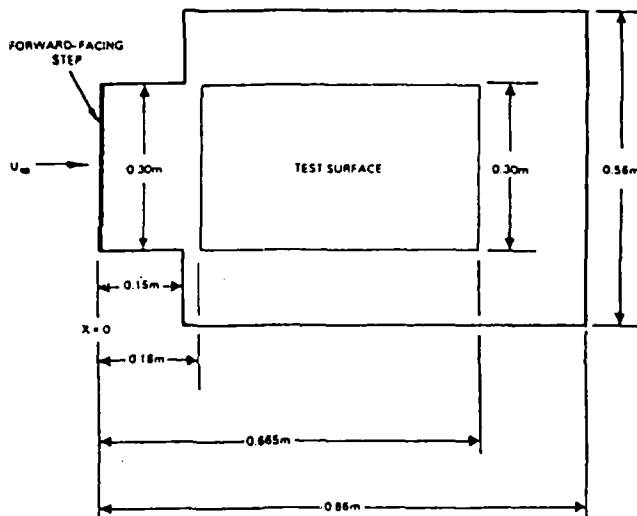


Figure 1: Test plate.



Figure 2: Photograph of riblet cross-section with  $h=s=0.003$  inch.

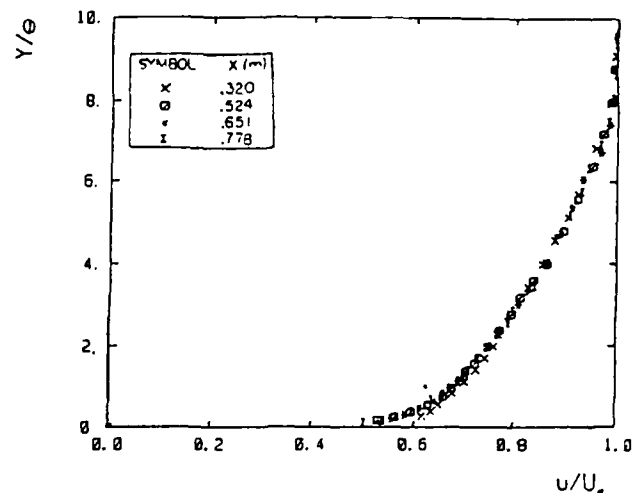


Figure 3: Reference velocity profiles (no riblets).

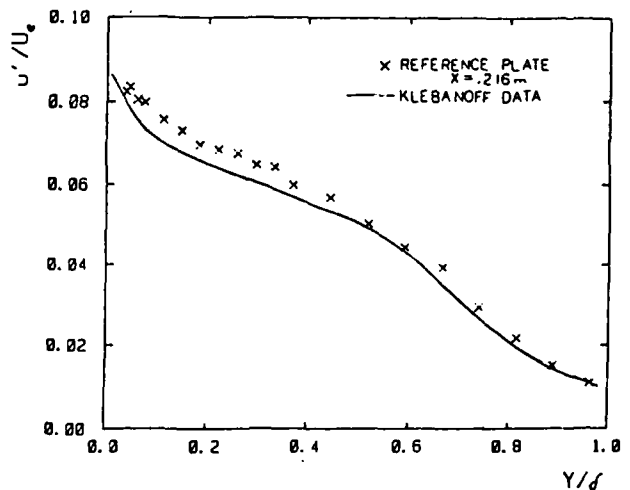


Figure 4: Profile of fluctuating streamwise velocity component (no riblets) compared to Klebanoff flat plate data.

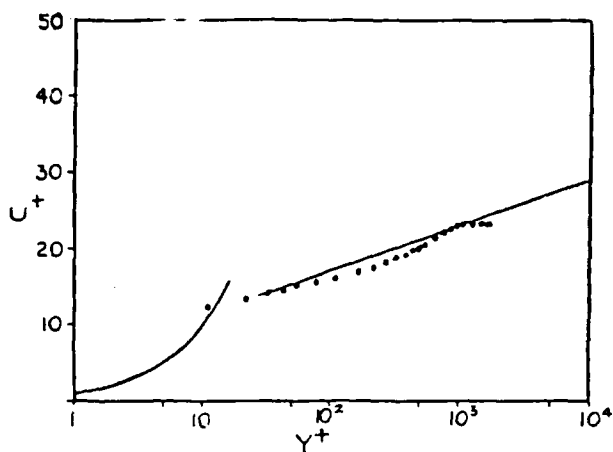


Figure 5: Reference data points (no riblets) compared to the Law of the Wall for  $x=0.179m$ .

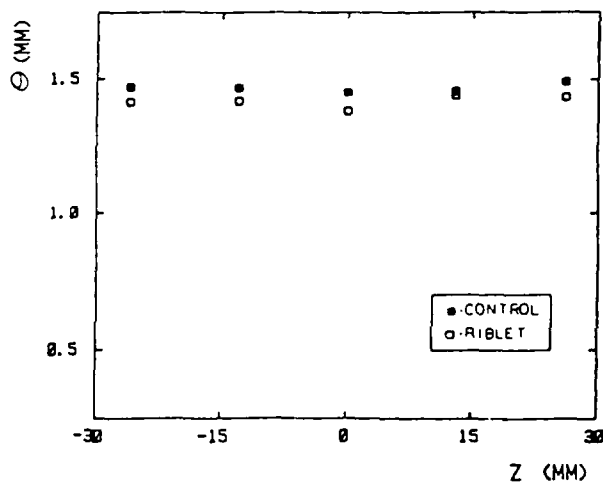


Figure 6: Momentum thickness ( $\theta$ ) vs. spanwise distance ( $z$ ), with and without riblets, for  $x=0.70m$ ,  $U_{\infty}=3.5m/sec$ ,  $s^+=13.1$ .

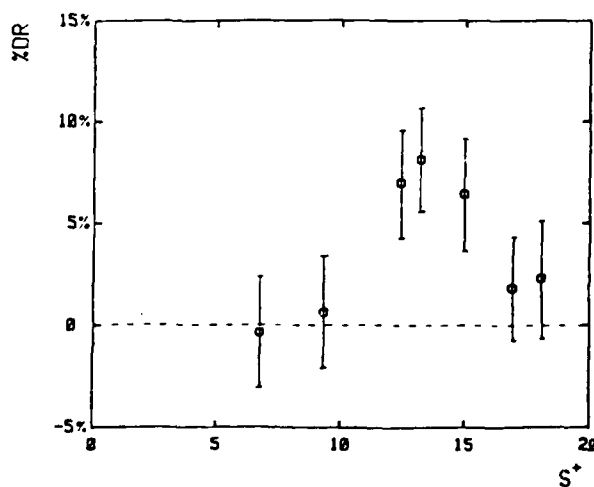


Figure 7: Percent drag reduction vs.  $s^+$  for 0.003 inch riblets.

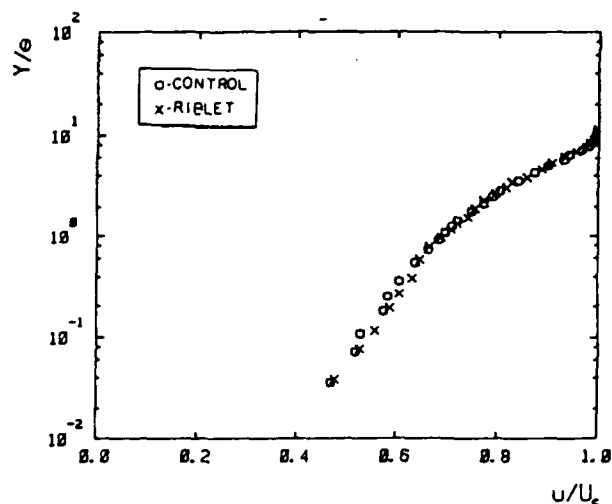


Figure 8: Mean streamwise velocity vs. distance above the plate, with and without riblets, for  $x=0.70m$ ,  $U_{\infty}=3.5m/sec$ ,  $s^+=13.1$ .

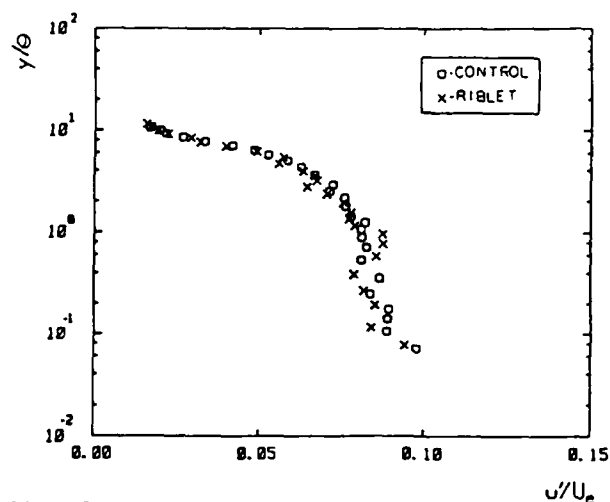


Figure 9: Fluctuating streamwise velocity component vs. distance above the plate, with and without riblets, for  $x=0.70m$ ,  $U_{\infty}=3.5m/sec$ ,  $s^+=13.1$ .

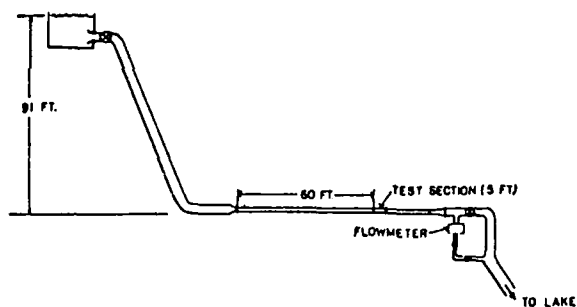


Figure 10: Schematic of 8-inch diameter pipe flow facility

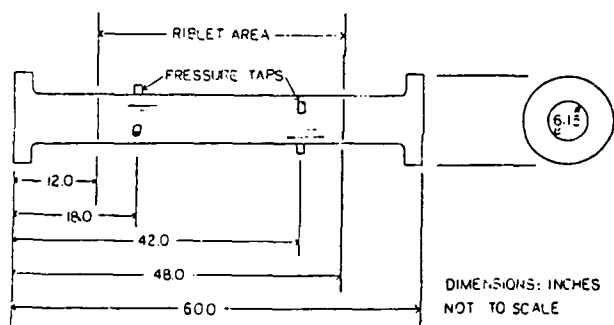


Figure 11: Schematic of pipe test section

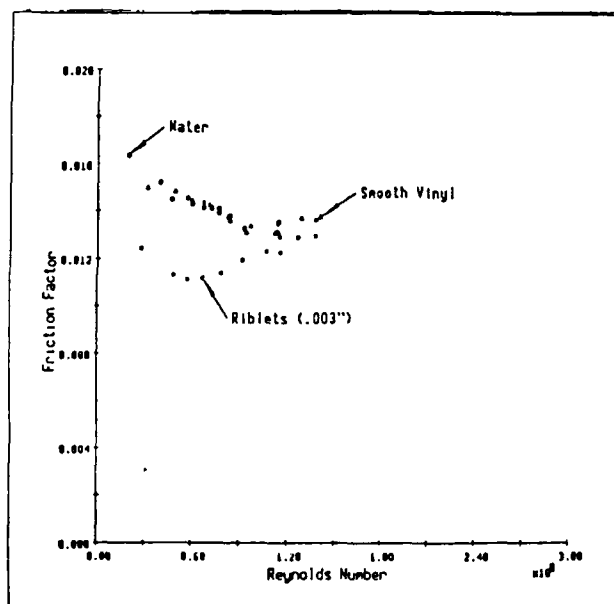


Figure 12:  $f$  versus  $Re_d$  for data set 1

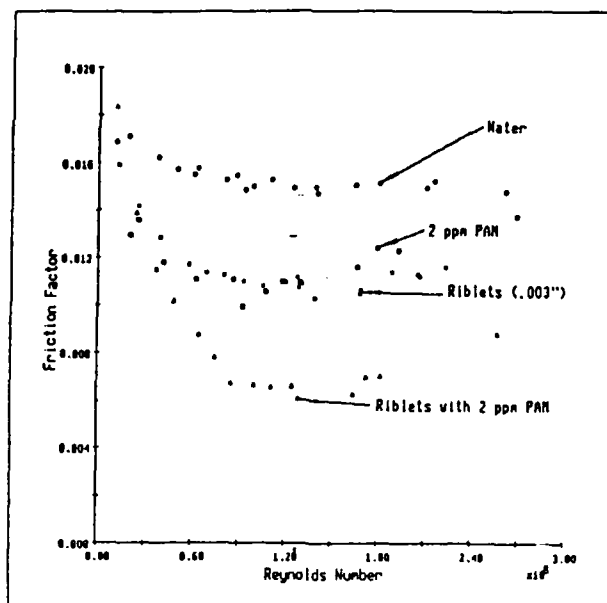


Figure 13:  $f$  versus  $Re_d$  for data set 2

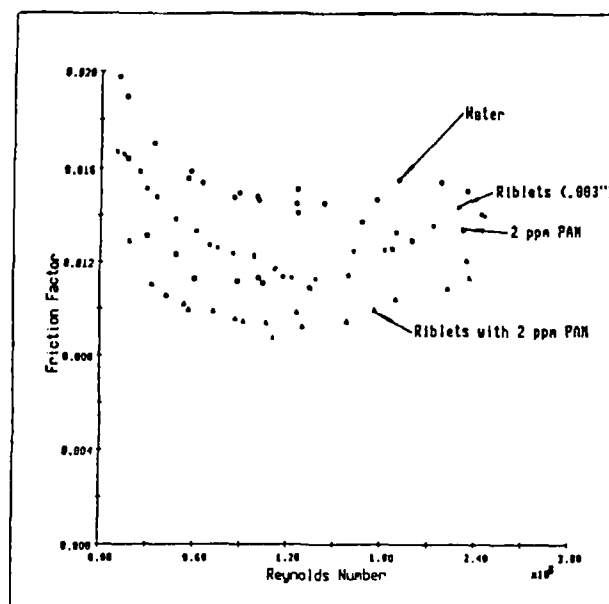


Figure 14:  $f$  versus  $Re_d$  for data set 3

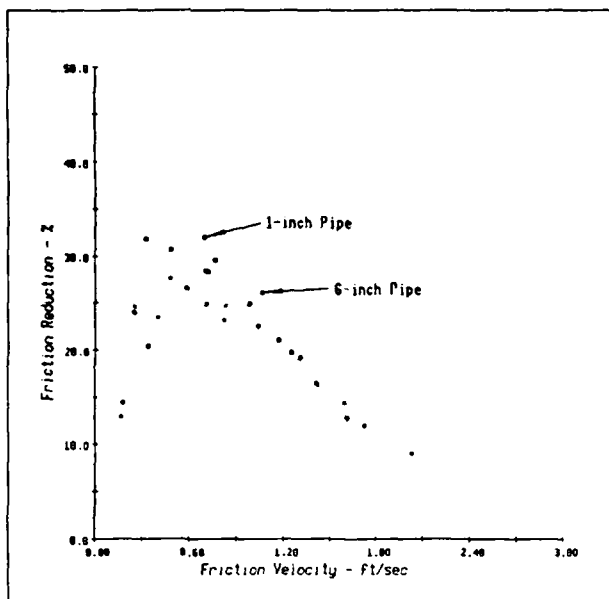


Figure 15: %DR versus  $u^*$  for 2ppm PAM in 1-inch and 6-inch diameter pipes

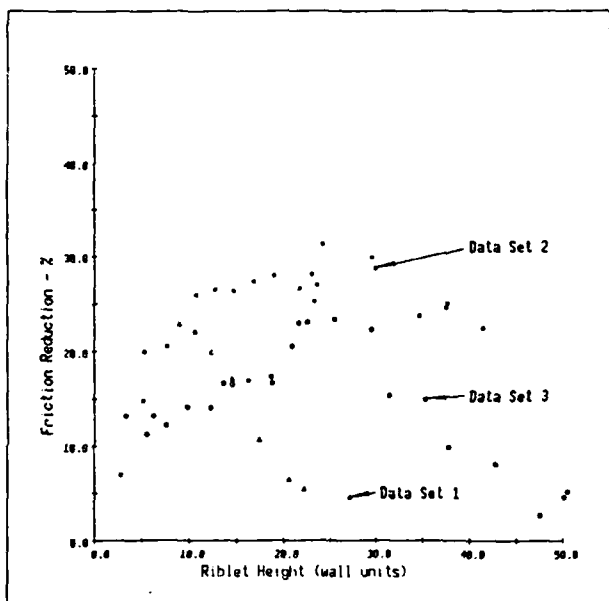


Figure 16: %DR versus  $s^+$  for data set 1,2, and 3 riblet tests

END

DATED

FILM

8-88

DTIC